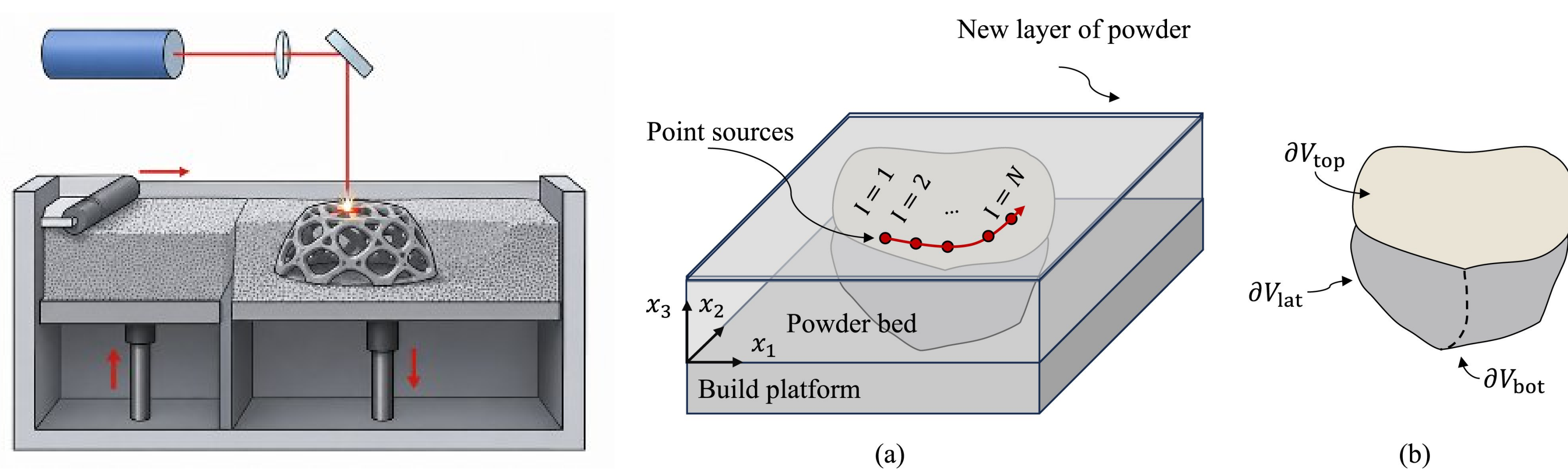


Introduction

Laser Powder Bed Fusion (LPBF) generates steep, fast-moving thermal gradients on the order of the laser spot radius $r_{\text{laser}} \approx 20 \mu\text{m}$. Conventional FEM requires either uniformly fine meshes or scan-wise adaptive remeshing — prohibitive at part scale. We present a **semi-analytical isogeometric framework** that:

- replaces the classical **image-source method** — which fails on realistic CAD — with an **IGA-discretised correction field**, enabling adiabatic BCs on arbitrary freeform geometries;
- delivers **80–258× CPU speed-up** over FEM at matched accuracy;
- is **heat-source agnostic**: the framework accommodates any analytical heat-source kernel admitting a half-space solution; demonstrated here with a Gaussian surface source.

LPBF Setup & Governing Equations



LPBF process: laser melts powder along a scan path.

Laser path discretised as N point sources; boundaries ∂V_{top} , ∂V_{lat} , ∂V_{bot} .

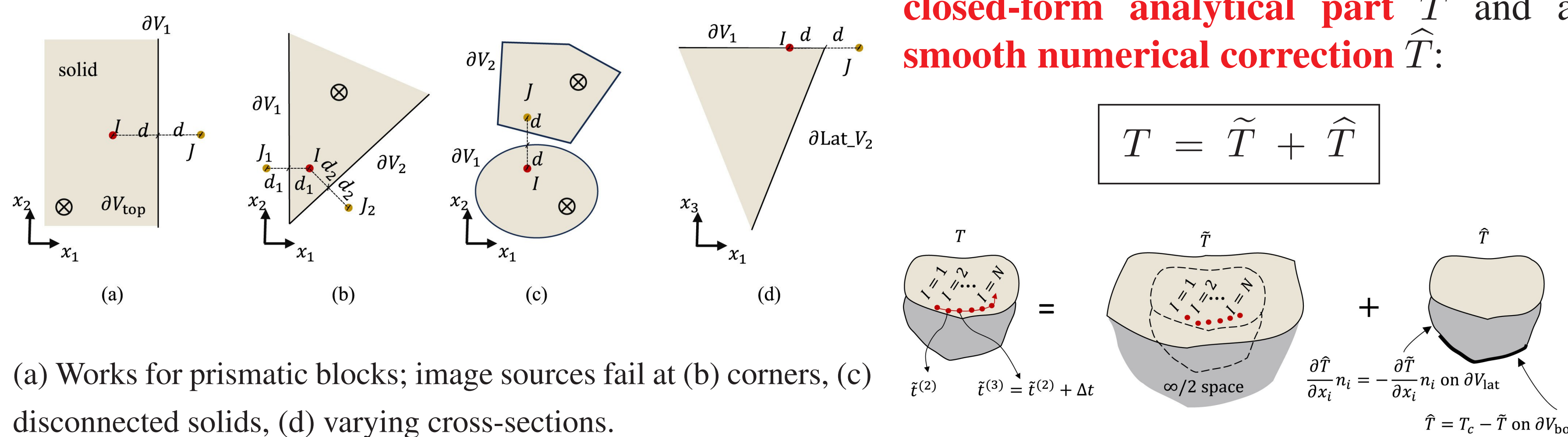
Heat equation. With density ρ , specific heat c_p , conductivity k , diffusivity $\alpha = k/(\rho c_p)$, and volumetric heat-source density Q , transient conduction in the build body V reads

$$\frac{\partial T}{\partial t} = \alpha \nabla^2 T + \frac{Q}{\rho c_p}, \quad \mathbf{x} \in V, t > 0, \quad \frac{\partial T}{\partial \mathbf{n}} = 0 \text{ on } \partial V_{\text{lat}} \cup \partial V_{\text{top}}, \quad T = T_c \text{ on } \partial V_{\text{bot}}, \quad (1)$$

with initial condition $T(\mathbf{x}, 0) = T_c$ (radiative and convective losses neglected at the top surface). The laser scan is discretised as N instantaneous point sources fired at shifted times $\tau^{(I)} = t^{(I)} - r^2/(8\alpha)$, which **exactly reproduces** a Gaussian surface source of radius r in the half-space; arc-length spacing $v \Delta t$, with $\Delta t = 1 \times 10^{-5}$ s.

Method: Analytical + Numerical Decomposition

Image-source method fails for realistic geometries: Our decomposition — split T into a **closed-form analytical part** \tilde{T} and a **smooth numerical correction** \hat{T} :



(a) Works for prismatic blocks; image sources fail at (b) corners, (c) disconnected solids, (d) varying cross-sections.

Analytical \tilde{T} — superposition of $K \leq N$ instantaneous point-source Green's functions in the half-space (early sources with negligible contribution at time t are truncated):

$$\tilde{T}(\mathbf{x}, t) = \sum_{I=1}^K \frac{E^{(I)}}{I \rho c_p [4\pi\alpha(t - \tau^{(I)})]^{3/2}} \exp\left(-\frac{\|\mathbf{x} - \mathbf{x}^{(I)}\|^2}{4\alpha(t - \tau^{(I)})}\right) H(t - \tau^{(I)}),$$

with absorbed pulse energy $E^{(I)} = AP\Delta t$ (absorptivity A , laser power P) and shifted activation $\tau^{(I)} = t^{(I)} - r^2/(8\alpha)$.

Correction \hat{T} — homogeneous heat equation with non-homogeneous BCs that compensate the half-space residual on the true geometry:

$$\rho c_p \frac{\partial \hat{T}}{\partial t} = k \nabla^2 \hat{T}, \quad \frac{\partial \hat{T}}{\partial \mathbf{n}} = -\frac{\partial \tilde{T}}{\partial \mathbf{n}} \text{ on } \partial V_{\text{lat}} \cup \partial V_{\text{top}}, \quad \hat{T} = T_c - \tilde{T} \text{ on } \partial V_{\text{bot}}.$$

Conclusions & References

- IGA correction \hat{T} enforces adiabatic BCs on realistic CAD geometries.
- C^{p-1} cubic NURBS retains $\leq 10\%$ error at elements $5\text{--}13 \times r_{\text{laser}}$.
- **80×** vs Abaqus C3D4, **258×** vs Abaqus C3D20 at matched accuracy.

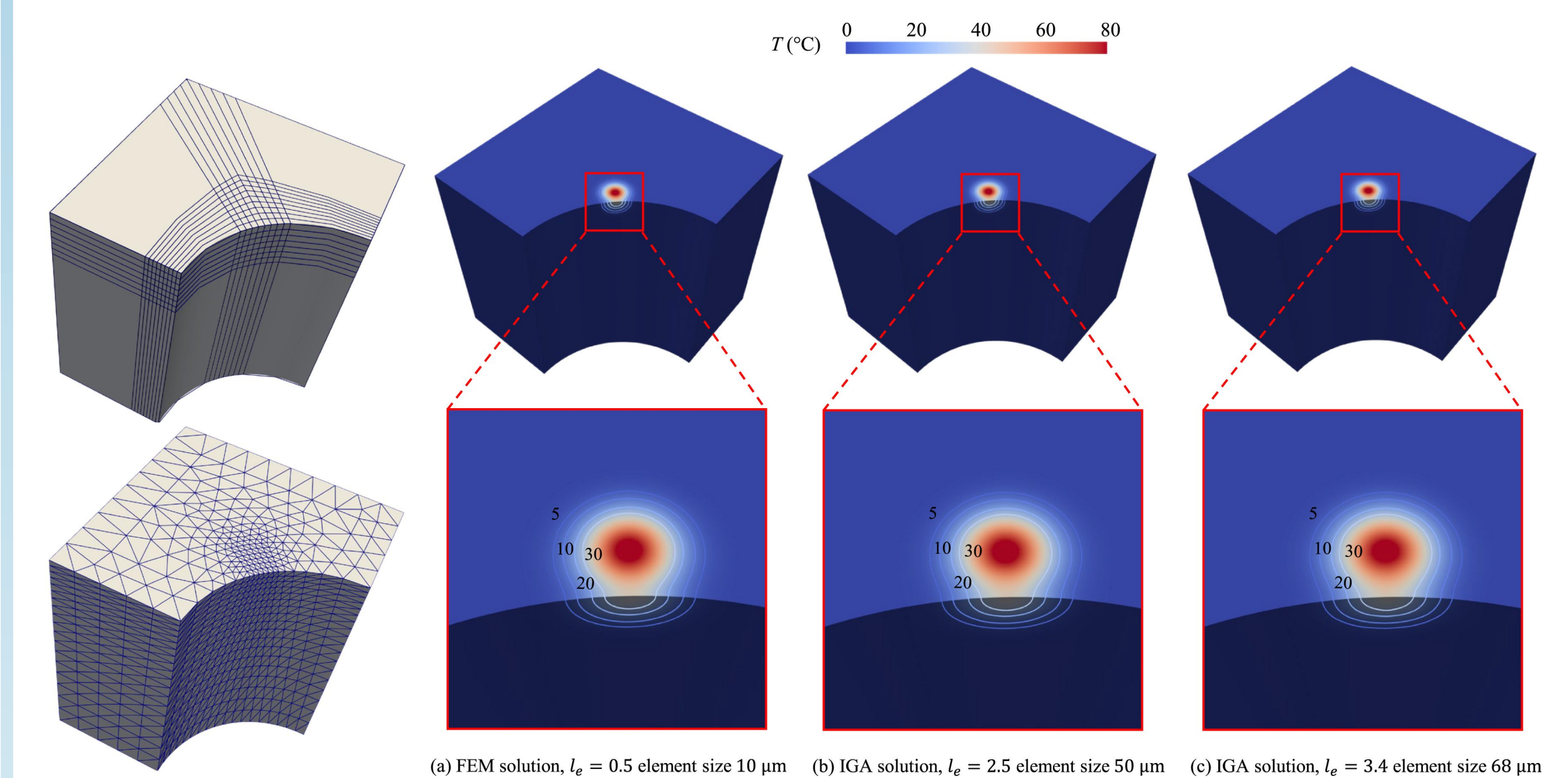
[1] Yang, Y., Ji, Y., Möller, M., & Ayas, C. (2026). Efficient thermal simulation in metal additive manufacturing via semi-analytical isogeometric analysis. *Computer Methods in Applied Mechanics and Engineering*, 457, 118992.

[2] Yang, Y., Ji, Y., Möller, M., & Ayas, C. (2025). Computational efficient process simulation of geometrically complex parts in metal additive manufacturing. *International Journal of Heat and Mass Transfer*, 248, 127059.

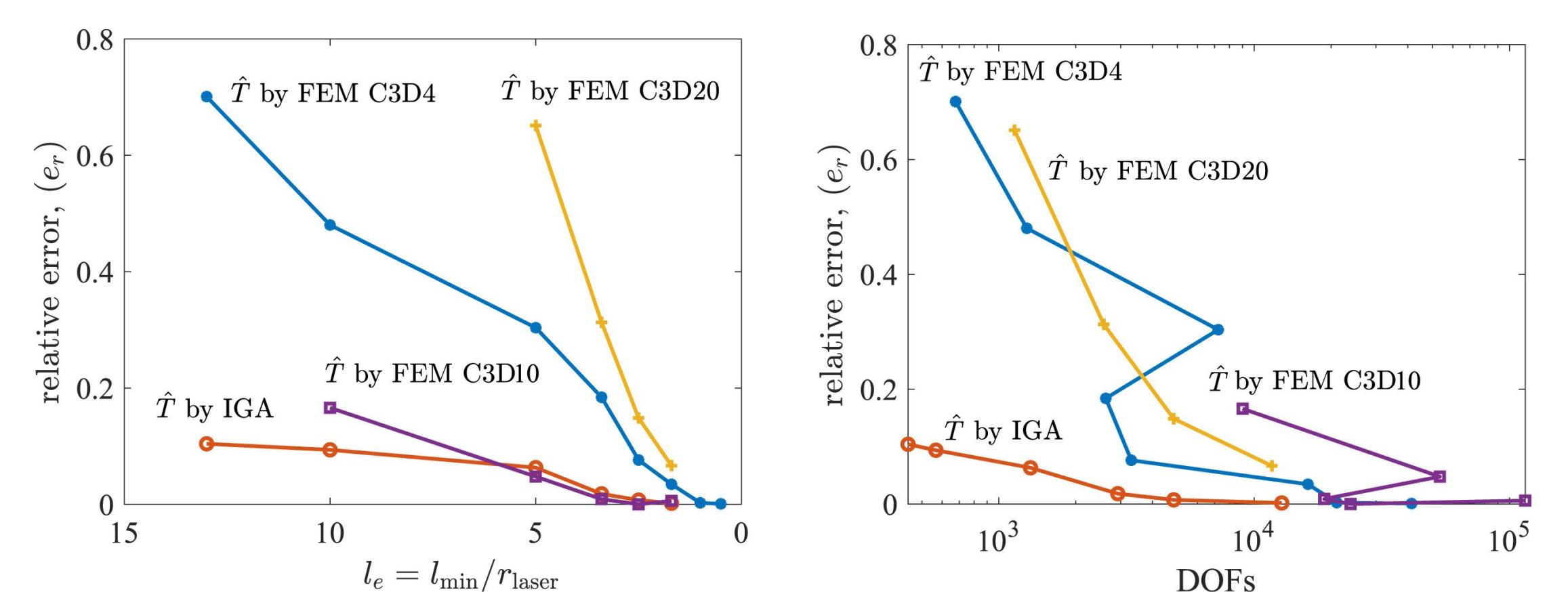
Convergence: Curved Boundary

Setup. 2 mm-edge cube with a quarter-cylinder ($R_c = 1$ mm) removed; point source $100 \mu\text{m}$ from the curved boundary. Ti-6Al-4V, $P = 82.5$ W, $A = 0.77$, $r_{\text{laser}} = 20 \mu\text{m}$. Mesh fineness reported as $l_e = l_{\text{min}}/r_{\text{laser}}$ (smaller = finer).

Temperature contours at matched coarse mesh $l_e = 3.4$: IGA reproduces the FEM reference ($l_e = 0.5$).



Convergence of the total field T in relative L^2 -error vs (a) element size l_e , (b) DOFs:



- **IGA retains $e_r \lesssim 10\%$ even at $l_e = 13$** — elements $13\times$ the laser radius;
- at matched DOFs: **1–2 orders of magnitude lower error** than FEM C3D4 / C3D20.

Thin-Wall: CPU Speed-up

Uniform mesh, target $e_r \leq 5\%$; FEM in Abaqus, IGA in G+Sm; Intel i7-11700 @ 2.5 GHz.

Method	$l_{\text{min}} [\mu\text{m}]$	DOFs	CPU/step [s]
IGA (quad.)	68	2639	0.132
Abaqus C3D4	20	11 536	10.625
Abaqus C3D20	20	45 261	34.043

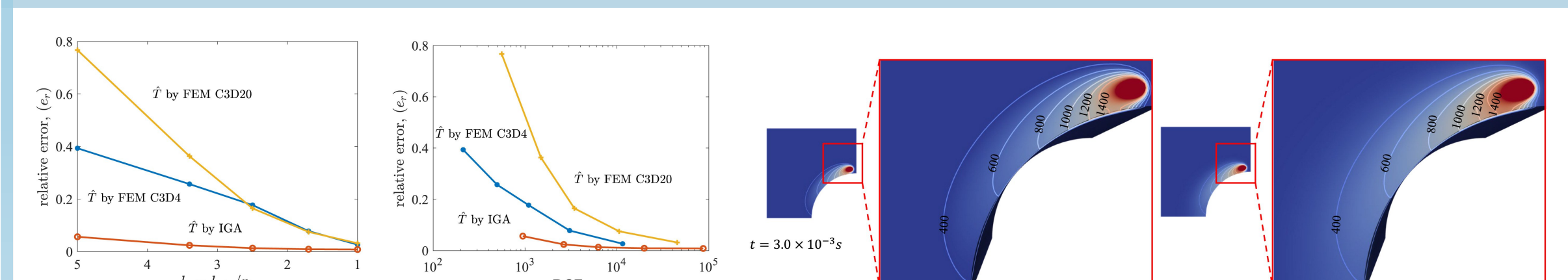
1 mm×0.2 mm×0.4 mm thin wall.

Speed-up at matched 5% error:

$$\frac{T_{\text{Abaqus, C3D4}}}{T_{\text{IGA}}} = \mathbf{80\times}, \quad \frac{T_{\text{Abaqus, C3D20}}}{T_{\text{IGA}}} = \mathbf{258\times}.$$

C^{p-1} -continuous NURBS represents through-thickness gradients smoothly across multiple elements, whereas C^0 FEM must reduce l_{min} to resolve the same gradient.

Contour Scan & Butterfly Part



Convergence of \hat{T} vs (a) l_e , (b) DOFs. Temperature contours; FEM ref ($l_e = 0.5$) vs IGA ($l_e = 5$).

Contour scan along curved boundary. At $t = 3 \times 10^{-3}$ s, the heat-flux residual (BC-violation measure on ∂V_{lat}): FEM 17.30% vs IGA's **8.03%** on a mesh **10× coarser** (5 415 vs 45 773 DOFs).

Butterfly part (cubic-NURBS volumetric parametrisation, IGA $l_e = 5$, **27 456 DOFs**) — adiabatic BCs on a free-form CAD surface, where the classical image-source method is **inapplicable**:

